

# A Model of Discharge Coefficient in Tertiary Box Combined with Overflow and Orifice

**Vena Rahayu Surya Putra**

Doctoral Program in Department of Water Resources, Faculty of Engineering, University of Brawijaya, Indonesia  
lilymont@ub.ac.id

**Mohammad Bisri**

Department of Water Resources, Faculty of Engineering, University of Brawijaya, Indonesia  
mbisri@ub.ac.id (corresponding author)

**Widandi Soetopo**

Department of Water Resources, Faculty of Engineering, University of Brawijaya, Indonesia  
widandi@ub.ac.id

**Moh Sholichin**

Department of Water Resources, Faculty of Engineering, University of Brawijaya, Indonesia  
mochsholichin@ub.ac.id

Received: 31 March 2025 | Accepted: 4 May 2025

Licensed under a CC-BY 4.0 license | Copyright (c) by the authors | DOI: <https://doi.org/10.48084/etasr.11230>

## ABSTRACT

This research investigates the effectiveness of tertiary boxes in irrigation systems by optimizing structural functions, combining overflow and orifice mechanisms to achieve more accurate water distribution. Designs incorporating overflow and orifice can achieve more balanced water allocation under various flow conditions. The discharge coefficient ( $C_d$ ) is measured due to variations in orifice number and diameter, and in the sharp-crested weir width. The results show that the discharge coefficient ( $C_d$ ) changes with variations in the width of the sharp-crested weir, indicating an accumulation or fluctuation along the weir width, diameter of orifice, and number of orifices. The optimal configuration between the discharge coefficient and the sharp-crested weir for sharp-crested weir widths of 0.33 m and 0.42 m was found, using 3 orifices, each with a diameter of 4 cm. The discharge coefficient over the sharp-crested weir for the width of 0.33 m uses the formula,  $C_d = 0.7384 (h_1/p) - 0.094$  for Channel-1 and  $C_d = 0.3294 \times (h_1/p) - 0.296$ , for Channel-2 and 3. The discharge coefficient on orifice uses the formula,  $C_d = 0.482 \times (h_1/d) - 0.0709$ , for Channel-1 and  $C_d = 0.3765 \times (h_1/d) \times 0.1751$ , for Channel-2 and 3. However, the discharge coefficient over the sharp-crested weir for the width of 0.42 m uses the formula,  $C_d = 0.8215 \times (h_1/p) - 0.058$ , for Channel-1 and  $C_d = 0.3202 \times (h_1/p) - 0.286$ , for Channel-2 and 3, the discharge coefficient on orifice uses the formula,  $C_d = 0.3469 \times (h_1/d) \times 0.2651$ , for Channel-1 and  $C_d = 0.177 \times (h_1/d) \times 0.614$  for Channel-2 and 3.

**Keywords-**discharge coefficient; orifice; overflow; physical model; model scenario

## I. INTRODUCTION

The tertiary box plays an important role in irrigation systems since it manages water distribution to agricultural areas. A side tertiary box often faces the problem of unbalanced flow because water, which has a straight flow, tends to have a bigger discharge [1] than that turned to the side. An alternative is a type of spear that is more accurate in dividing water proportionally but requires a bigger area [2].

The orifice overflow (sharp-crested weir) structure [3-4] has been developed as a contemporary solution. This design uses the holes in overflow (sharp-crested weir) side [5] to

increase the effectiveness of water distribution [6]. With a higher discharge coefficient, this structure is more effective in regulating water flow [7-8]. The combination of overflow and orifice [9-10] is also introduced as a flexible alternative for regulating water discharge in various flow conditions, giving more proportional water distribution [11] without needing additional space. This solution is expected to help modernize irrigation, make operation easier, and provide reliable irrigation service for farmers [12-15].

This study provides water allocation values, a combination of structures, and discharge coefficients for three flow

directions using overflow and orifice, as well as the dimensions and position of the orifice to optimize water allocation. However, more emphasis is placed on the measurement of the discharge coefficient ( $C_d$ ) of the tertiary box combined with overflow and orifice. To obtain the flow value, a simulation is needed, using the number and diameter of orifices along with the observed discharge [16], water level, and flow velocity on the orifice. This study provides a reference for implementing a laboratory practice. This study is usually carried out to find the value of the discharge coefficient, which is useful as an initial step for the design of sharp overflow (sharp-crested weir) structures combined with overflow and orifice, or other structures.

II. MATERIALS AND METHODS

A. Rectangular Notch

According to [17], a rectangular notch is formed when water flows through a rectangular shaped gap, as shown in Figure 1. The  $H$  variable, observed in Figure 1, demonstrates the water overflow height and  $b$  shows the overflow width.

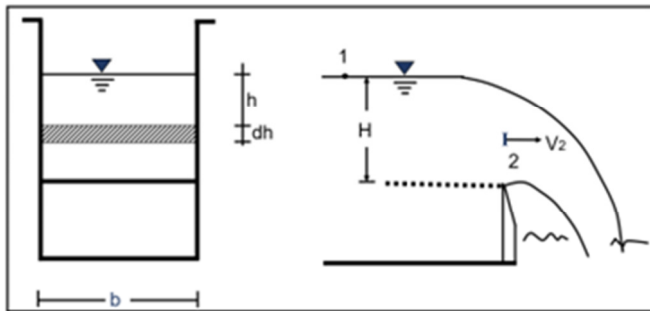


Fig. 1. Rectangular notch as described in [17].

To calculate the total discharge through the whole overflow, an analysis using integral equation (1) is needed, from  $h = 0$  at the water level until  $h = H$  at the overflow peak:

$$Q_{th} = \frac{2}{3} \times C_d \times b \times \sqrt{2g} \times H^{\frac{3}{2}} \tag{1}$$

Where,  $Q_{th}$  = theoretical flow discharge ( $m^3$ /hour),  $g$  = acceleration due to gravity ( $m/s^2$ ),  $b$  = width of rectangular notch (m),  $C_d$  = discharge coefficient,  $h$  = height of section from water level (m).

B. Calculation of Flow Coefficient

Liquid flowing through the orifice (Figure 1) arrives from all directions. Due to the liquid's viscosity, particles that change direction experience energy losses [18–19]. After passing through the jet hole, water undergoes contraction, as shown by the flow contraction in Figure 2. The maximum contraction happens in a section that is downstream side. The section with the maximum contraction is known as Vena Contracta.

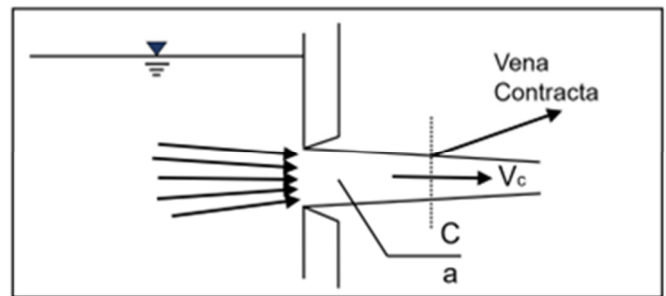


Fig. 2. Illustration of Vena Contracta.

In liquid flowing through a hole, energy losses occur that cause some flow parameters to be less than those of ideal liquid flow. This can be shown by several coefficients: contraction, velocity, and discharge coefficients.

The coefficient of contraction ( $C_c$ ) is the ratio between the section area of the flow in the vena construct ( $A_c$ ) and the hole area ( $a$ ), which is the same with the flow section of the ideal liquid. The coefficient of contraction ( $C_c$ ) can be calculated using:

$$C_c = \frac{A_c}{a} \tag{2}$$

The contraction coefficient ( $C_c$ ) depends on the energy head, shape of the hole, size of hole, and the average is taken as 0.64.

The ratio between real velocity in the vena construct ( $V_c$ ) and theoretical velocity ( $V$ ) is known as velocity coefficient ( $C_v$ ) and it can be calculated as:

$$C_v = \frac{V_c}{V} \tag{3}$$

The value of the velocity coefficient depends on the shape of the underside of the hole (sharp or rounded) and the energy head. The average of the velocity coefficient,  $C_v$ , is taken as 0.97.

The discharge coefficient is the ratio between the real discharge and the theoretical discharge and it can be calculated as:

$$C_d = C_v \times C_c \tag{4}$$

The value of the discharge coefficient depends on the value of  $C_c$  and  $C_v$ , and is taken as 0.62.

C. Small Hole

Figure 3 shows the liquid that flows through the small hole of a tank. The center of the hole is at a distance  $h$  from the water level. At first, the flow is assumed to be ideal and the pressure in the hole is atmospheric pressure.

By using the Bernoulli equation in the liquid surface in poll and hole, the velocity of the liquid in the point can be calculated as [20]:

$$Z_1 + \frac{P_1}{\gamma} + \frac{V_1^2}{2g} = Z_2 + \frac{P_2}{\gamma} + \frac{V_2^2}{2g} \tag{5}$$

The velocity in point-1 is zero and the pressure is the same, so (5) can be written as:

$$Z_1 = Z_2 + \frac{v_2^2}{2g} \tag{6}$$

$$V_2 = 2g(Z_1 + Z_2) = 2gh \tag{7}$$

Or:

$$V_2 = \sqrt{2gh} \tag{8}$$

The equation shows the theoretical flow velocity of the ideal liquid. In real liquids, energy losses occur due to viscosity, resulting in the Vena Contracta phenomenon. Therefore, the velocity coefficient ( $C_v$ ) must be calculated as:

$$V_c = C_v \times V_2 = C_v \times \sqrt{2gh} \tag{9}$$

Hence, the discharge can be calculated as:

$$Q = A_c \times V_c = C_c \times a \times C_v \times \sqrt{2gh} \tag{10}$$

Or:

$$Q = C_d \times a \times \sqrt{2gh} \tag{11}$$

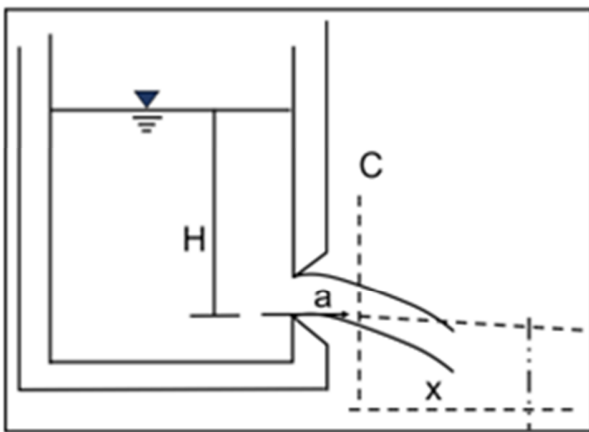


Fig. 3. Illustration of tank with a small hole.

### III. METHODOLOGY

#### A. Data Collection

The collected data include the Thompson head ( $h_t$ ), the pitot head ( $h_p$ ) within the orifice, and the water surface head over the sharp-crested weir. Then, the data are analyzed to obtain the constant discharge coefficient. The results of this analysis are used to address the problem formulation by examining how variations in orifice diameter and number influence the discharge coefficient ( $C_d$ ) in water allocation within the tertiary box with three flow directions.

#### B. Experimental Procedure

The experimental procedure consisted of the following steps:

- Installing the rectangular notch and activating the water pump to start the flow through the channel.
- Measuring Thompson gauge reading, Pitot height  $h$  in the orifice, and water level head in sharp-crested weir.

- The discharge measurement process employed two methods (Thompson and Pitot), which were used to calculate the total discharge as well as the discharge coefficient ( $C_d$ ) for the sharp-crested weir.
- The calculation of  $Q_{Thompson}$  from  $h_{Thompson}$  is performed to obtain discharge, which is based on the Thompson measuring tool. Subsequently,  $V_{pitot}$  is calculated from  $h$  Pitot in the orifice, which is subsequently used to calculate the discharge coefficient of a free flow orifice ( $C_d$ ). This is then followed by the calculation of  $Q_{orifice}$ . After that, the discharge through the sharp-crested weir is calculated with the equation,  $Q_{sharp-crested\ weir} = Q_{Thompson} - Q_{orifice}$  by using the calculation of orifice discharge coefficient. After  $Q_{sharp-crested\ weir}$  is known, the next step is the discharge coefficient ( $C_d$ ) calculation through the sharp-crested weir.

#### C. Location

This research is conducted in the Laboratory of Applied Hydraulics, Department of Water Resources, Faculty of Engineering, University of Brawijaya.

#### D. Study Scope

This research measures the discharge coefficient and design parameter of tertiary box structure combined with overflow and orifice that is more efficient in terms of water allocation accuracy. So, the water allocation service in the irrigation network can be performed optimally.

#### E. Physical Model

The physical model tested in this study is a tertiary box model featuring three flow directions, incorporating both overflow and orifice mechanisms. The model scale [21] is a prototype scale of 1:1. The model construction is designed with a flume/open channel.

## IV. RESULTS AND DISCUSSION

In this study, eight variations of discharge, three variations of orifice diameter, two variations of sharp-crested weir width, and two variations of orifice number are used. From the calculation and direct measurements across various orifice combination scenarios, it was found that the water level height at the sharp-crested weir sometimes resulted in overflow and sometimes did not. For example, in the scenario with an orifice diameter of 8 cm, three orifices, and a sharp-crested weir width of 0.33 m, there is no overflow at discharges of 25-45 l/s. However, overflow occurs at discharges of 50-60 l/s.

TABLE I. CALCULATION OF  $C_d$  OVER SHARP-CRESTED WEIR WITHOUT ORIFICE

No.	$Q_{Thompson}$ m <sup>3</sup> /dt	$h$ m	$b$ m	$C_d$
1	0.009	0.046	0.33	0.959
2	0.011	0.054	0.33	0.926
3	0.014	0.064	0.33	0.899
4	0.016	0.072	0.33	0.870
5	0.018	0.078	0.33	0.855
6	0.020	0.086	0.33	0.815
7	0.023	0.095	0.33	0.795
8	0.025	0.105	0.33	0.762
Mean				0.860



Fig. 4. Orifice on the sharp-crested weir.



Fig. 5. Overflow condition in the sharp-crested weir without orifice.

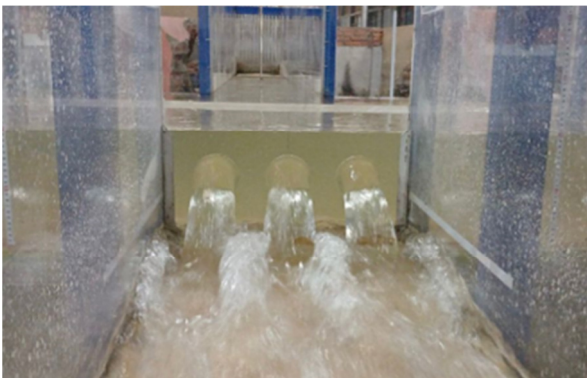


Fig. 6. Non-overflow condition in the sharp-crested weir combined with orifice.



Fig. 7. Overflow condition in the sharp-crested weir combined with orifice.

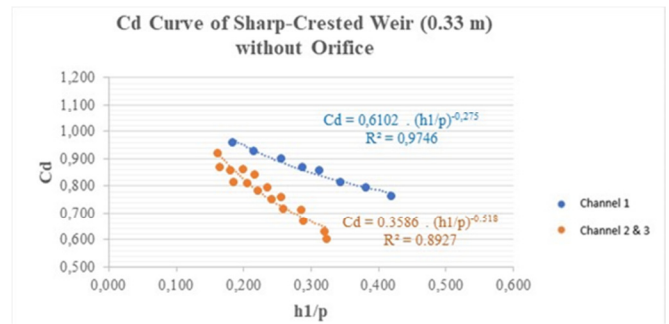


Fig. 8.  $C_d$  curve of sharp-crested weir (0.33 m) without orifice.

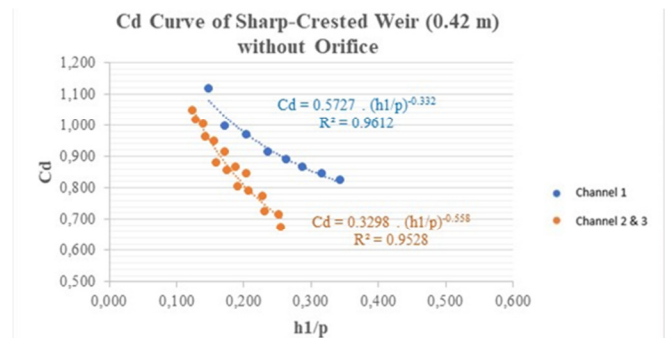


Fig. 9.  $C_d$  curve of sharp-crested weir (0.42 m) without orifice.

Based on the measurements of  $h_{Thompson}$  and the water level over the sharp-crested weir, the discharge coefficient over the sharp-crested weir is analyzed for the scenario without an orifice.

$$Q = \left( \frac{h_{Thompson}}{0.8153} \right)^{\frac{1}{0.3893}} \Rightarrow h_{Thompson} = 0.132 \text{ m}$$

$$Q = \left( \frac{0.132}{0.8153} \right)^{\frac{1}{0.3893}} \Rightarrow Q = 0.009 \text{ m}^3/\text{s}$$

The next step is to analyze the discharge coefficient over the sharp-crested weir:

$$Q = \frac{Q_{thompson}}{\frac{2}{3} \times b \times \sqrt{2 \times g \times h^2}}$$

Or:

$$C_d = \frac{0.009}{\frac{2}{3} \times 0.33 \times \sqrt{2 \times 9.81 \times 0.046^2}} \Rightarrow C_d = 0.959$$

For a sharp-crested weir combined with an orifice, two discharge coefficients are calculated when overflow occurs. Based on the measurement of  $h_{Thompson}$ ,  $h_{pilot}$  in the orifice, and the water level over the sharp-crested weir, the discharge coefficient over the sharp-crested weir and the discharge coefficient in the orifice are analyzed. In the scenario presented in Tables II and III: the orifice diameter is 8 cm, there are 3 orifices, and the sharp-crested weir width is 0.33 m in Channel-1. The first step in this analysis is to calculate the discharge of Thompson by using the calibration formula of  $Q_{Thompson}$  :

$$Q = \left( \frac{h_{thompson}}{0.8153} \right)^{\frac{1}{0.3893}} \Rightarrow h_{Thompson} = 0.135 \text{ m}$$

$$Q = \left( \frac{0.135}{0.8153} \right)^{\frac{1}{0.3893}} \Rightarrow Q = 0.010 \text{ m}^3/\text{s}$$

Analysis of discharge coefficient ( $C_d$ ) in the orifice:

$$C_V = 1.019$$

$$C_C = 0.64 \Rightarrow C_C \text{ mean} = 0.64$$

$$C_{d\text{-orifice}} = C_V \times C_C \Rightarrow C_{d\text{-orifice}} = 0.652$$

$$Q_{\text{orifice}} = C_d \times a \times \sqrt{2 \times g \times h}$$

Or:

$$Q = 0.652 \times 0.005 \times \sqrt{2 \times 9.81 \times 0.049}$$

$$Q_{\text{orifice}} = 0.003 \text{ m}^3/\text{s}$$

$$Q_{\text{total orifice}} = 0.003 \text{ m}^3/\text{s}$$

$$Q_{\text{total orifice}} = 0.0010 \text{ m}^3/\text{s}$$

From the total discharge of the orifice, the discharge coefficient over the sharp-crested weir can be calculated. The value of the discharge coefficient over the sharp-crested weir is calculated using the discharge from  $Q_{\text{Thompson}}$  and  $Q_{\text{total orifice}}$  :

$$Q_{\text{Thompson}} = 0.020 \text{ m}^3/\text{s}$$

$$Q_{\text{orifice}} = Q_{\text{total orifice}}$$

$$Q_{\text{orifice}} = 0.014 \text{ m}^3/\text{s}$$

$$Q_{\text{sharp-crested weir}} = Q_{\text{Thompson}} - Q_{\text{total orifice}}$$

$$Q_{\text{sharp-crested weir}} = 0.020 - 0.014$$

$$Q_{\text{sharp-crested weir}} = 0.006 \text{ m}^3/\text{s}$$

$$h = 0.026$$

$$b = 0.33 \text{ m}$$

$$C_{\text{sharp crested weir}} = \frac{Q_{\text{weir}}}{\frac{2}{3} \times b \times \sqrt{2 \times g \times h^2}}$$

$$C_{\text{sharp-crested weir}} = \frac{0.006}{\frac{2}{3} \times 0.33 \times \sqrt{2 \times 9.81 \times 0.026^2}}$$

$$C_{\text{sharp crested weir}} = 1.52$$

A summary of the mean  $C_d$  from various sharp-crested weir scenarios (0.33 m and 0.42 m) is provided in Tables IV and V.

TABLE II. ANALYSIS OF DISCHARGE COEFFICIENT IN ORIFICE

h m	d m	A m <sup>2</sup>	h <sub>1</sub> /d	V <sub>actual</sub> m/s	T <sub>theoretical</sub> m/s	C <sub>V</sub>	C <sub>C</sub>	C <sub>d</sub>	Q <sub>every orifice</sub>	Q <sub>total orifice</sub>	
0.049	0.08	0.005	0.608	0.995	0.977	1.019	0.64	0.652	0.003	0.010	
0.067	0.08	0.005	0.833	1.123	1.144	0.982	0.64	0.629	0.004	0.011	
0.075	0.08	0.005	0.933	1.190	1.210	0.983	0.64	0.629	0.004	0.011	
0.102	0.08	0.005	1.275	1.257	1.415	0.888	0.64	0.569	0.004	0.012	
0.123	0.08	0.005	1.538	1.347	1.553	0.867	0.64	0.555	0.004	0.013	
0.156	0.08	0.005	1.950	1.441	1.749	0.824	0.64	0.527	0.005	0.014	
0.166	0.08	0.005	2.075	1.504	1.805	0.833	0.64	0.533	0.005	0.015	
0.170	0.08	0.005	2.125	1.554	1.826	0.851	0.64	0.545	0.005	0.015	
Mean									0.580	0.004	0.013

TABLE III. ANALYSIS OF DISCHARGE COEFFICIENT OVER THE SHARP-CRESTED WEIR COMBINED WITH ORIFICE

No.	Q <sub>Thompson</sub> m <sup>3</sup> /dt	Q <sub>orifice</sub>	Q <sub>sharp-crested weir</sub> m <sup>3</sup> /s	h m	b m	p m	h <sub>1</sub> /p	C <sub>d</sub>	
1	0.010	0.010	-	-	0.33	0.25	-	-	
2	0.012	0.011	-	-	0.33	0.25	-	-	
3	0.013	0.011	-	-	0.33	0.25	-	-	
4	0.017	0.012	-	-	0.33	0.25	-	-	
5	0.018	0.013	-	-	0.33	0.25	-	-	
6	0.020	0.014	0.006	0.026	0.33	0.25	0.104	1.522	
7	0.022	0.015	0.008	0.036	0.33	0.25	0.144	1.172	
8	0.025	0.015	0.010	0.040	0.33	0.25	0.160	1.338	
Mean									1.344

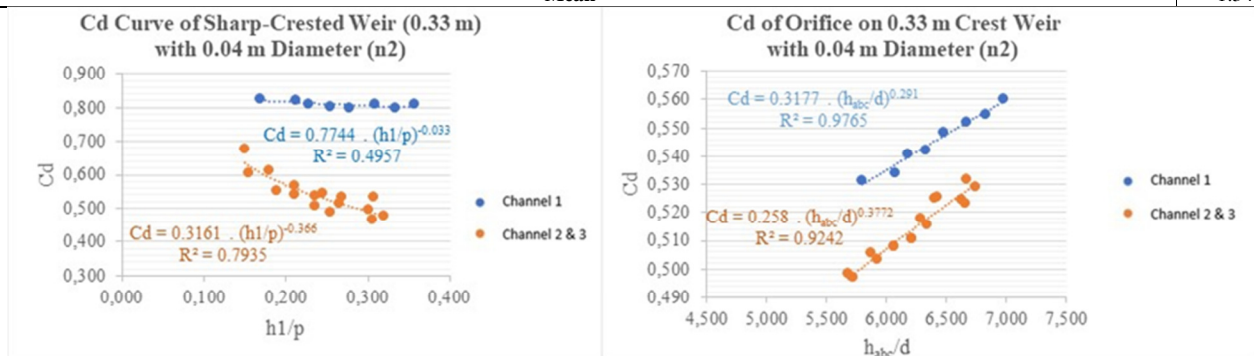


Fig. 10. C<sub>d</sub> curve for sharp-crested weir and Cd for orifice (D4 n2) – sharp-crested weir (0.33 m).

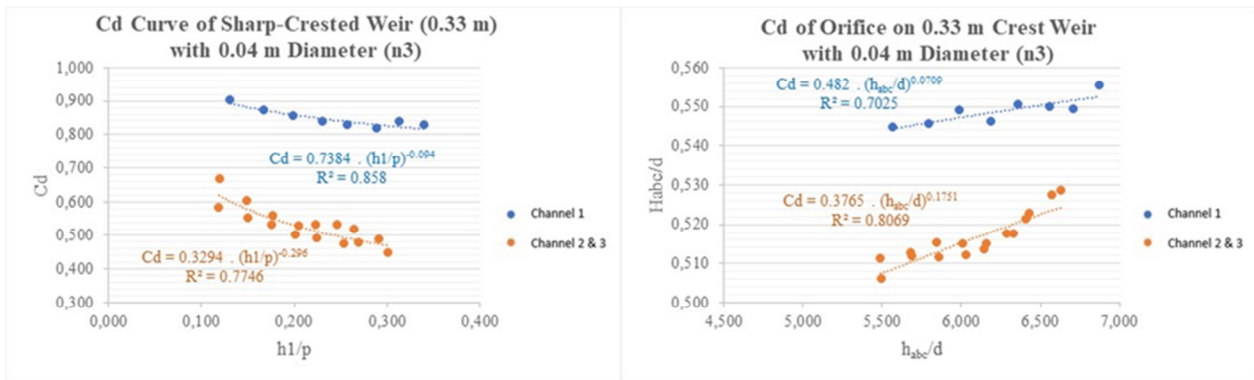


Fig. 11.  $C_d$  curve for sharp-crested weir and Cd for orifice (D4 n3) – sharp-crested weir (0.33 m).

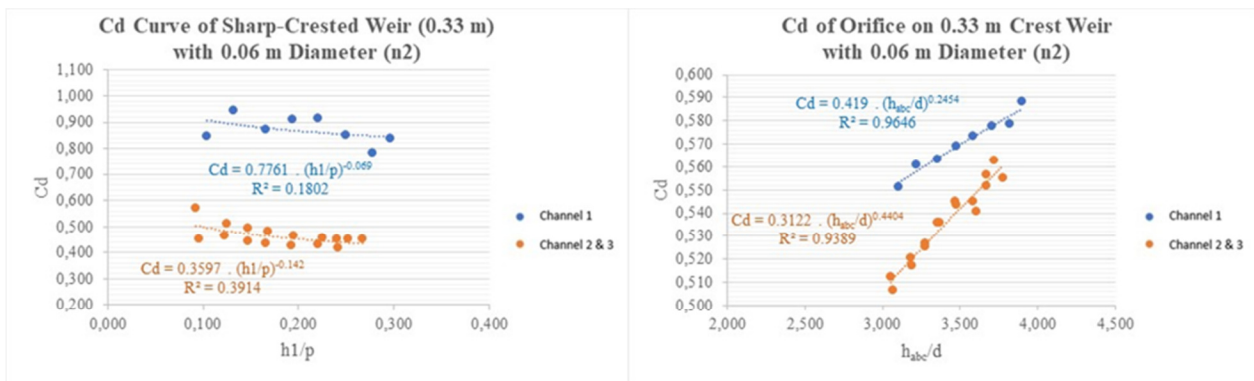


Fig. 12.  $C_d$  curve for sharp-crested weir and Cd for orifice (D6 n2) – sharp-crested weir (0.33 m).

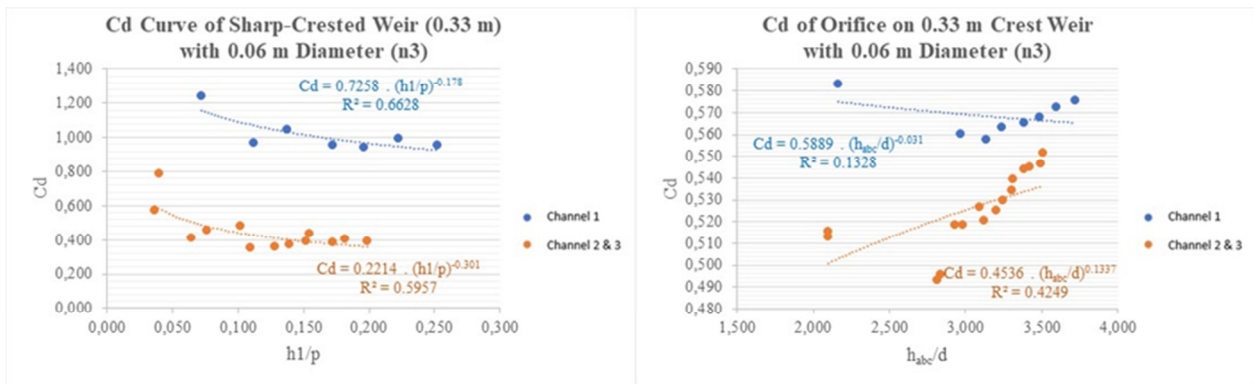


Fig. 13.  $C_d$  curve for sharp-crested weir and Cd for orifice (D6 n3) – sharp-crested weir (0.33 m).

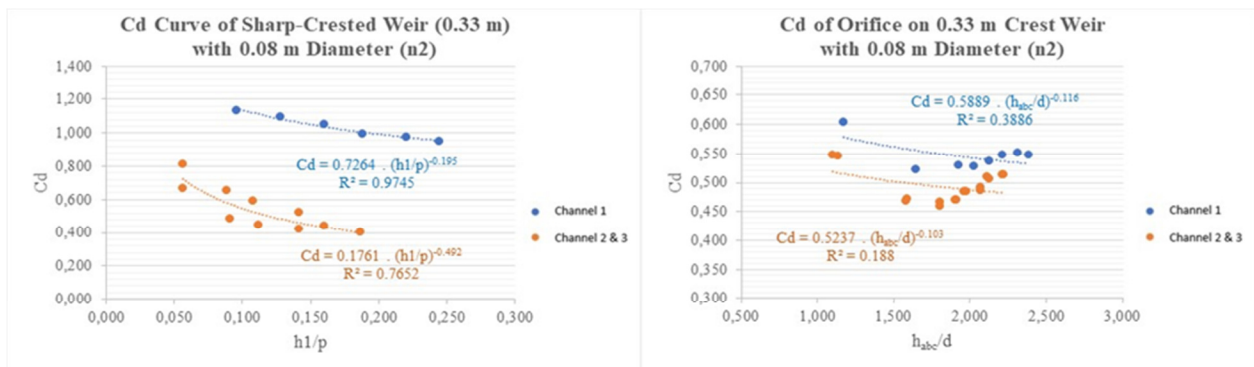


Fig. 14.  $C_d$  curve for sharp-crested weir and Cd for orifice (D8 n2) – sharp-crested weir (0.33 m).

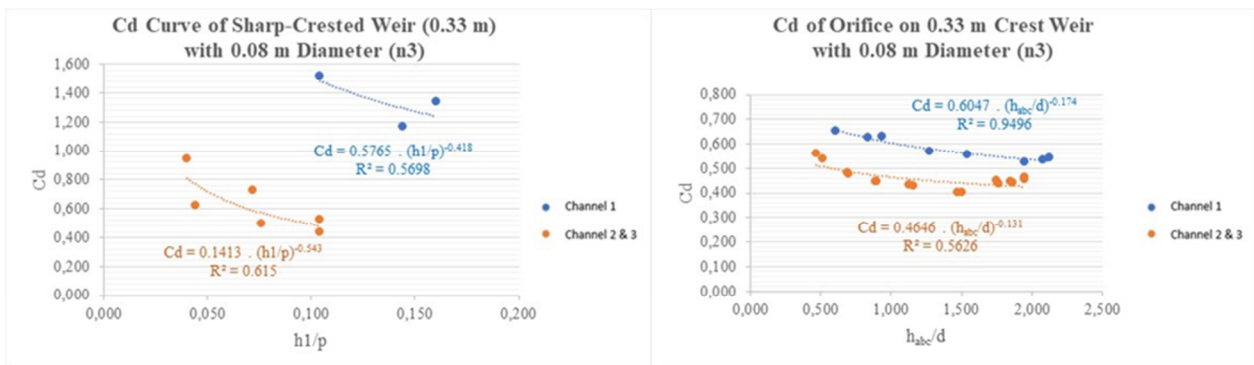


Fig. 15.  $C_d$  curve for sharp-crested weir and Cd for orifice (D8 n3) – sharp-crested weir (0.33 m).

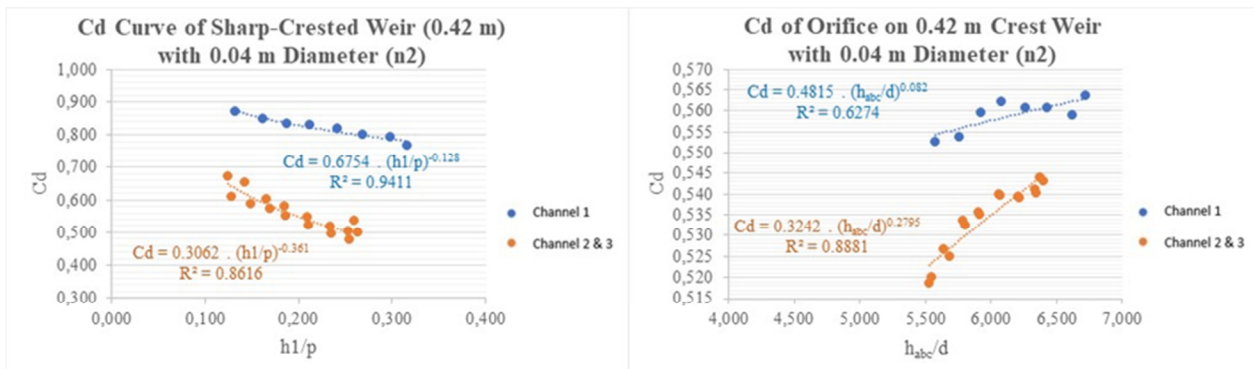


Fig. 16.  $C_d$  curve for sharp-crested weir and Cd for orifice (D4 n2) – sharp-crested weir (0.42 m).

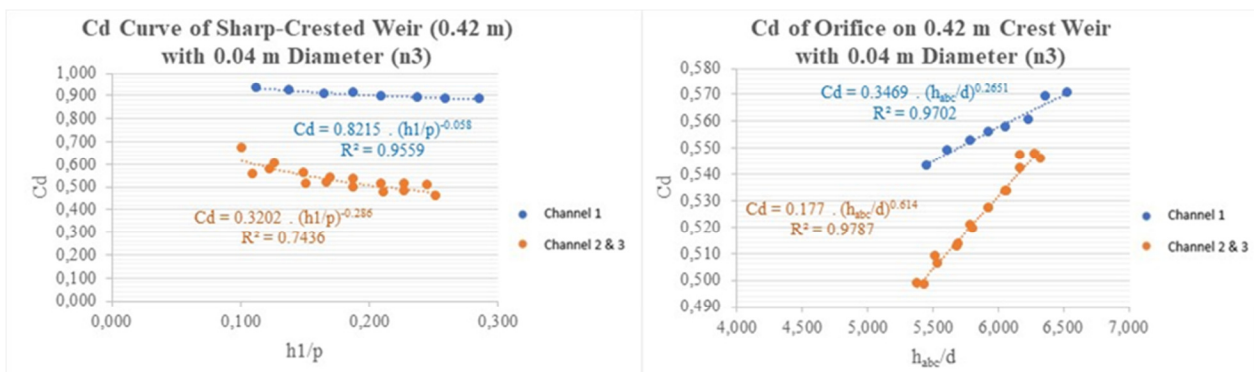


Fig. 17.  $C_d$  curve for sharp-crested weir and Cd for orifice (D4 n3) – sharp-crested weir (0.42 m).

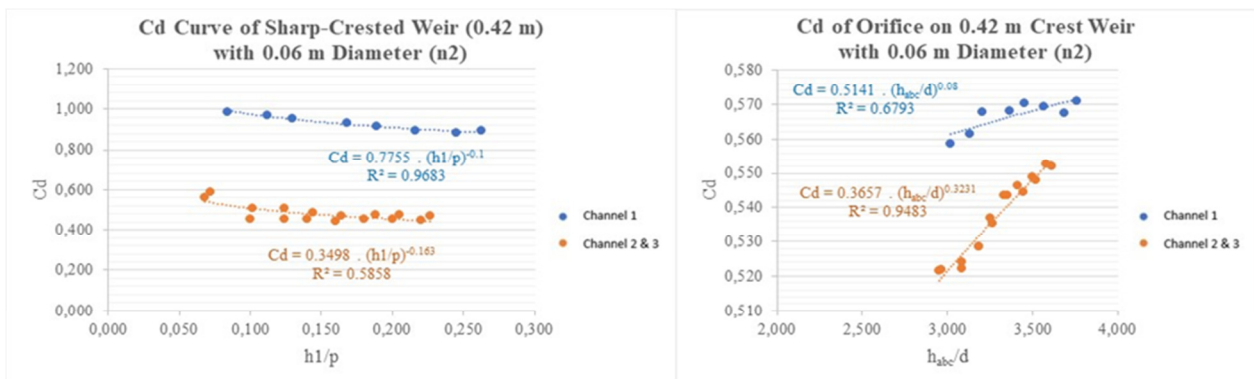


Fig. 18.  $C_d$  curve for sharp-crested weir and Cd for orifice (D6 n2) – sharp-crested weir (0.42 m).

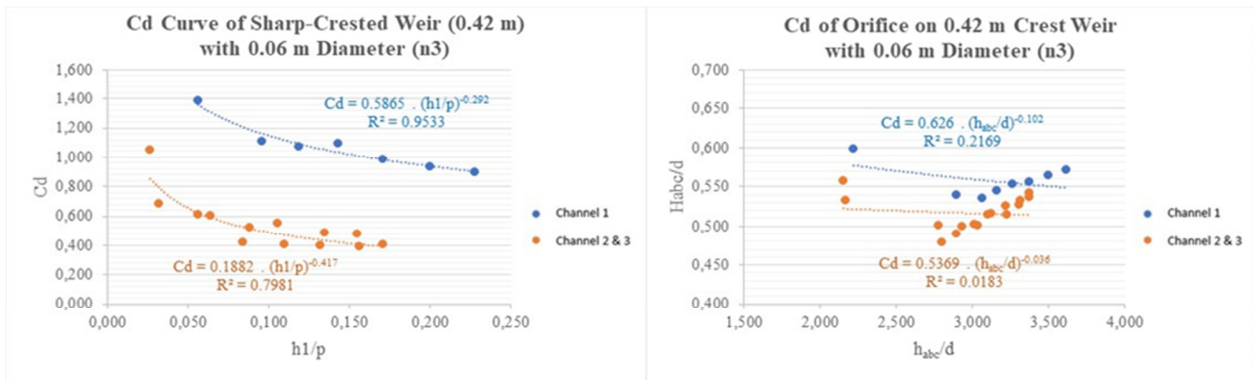


Fig. 19.  $C_d$  curve for sharp-crested weir and  $C_d$  for orifice (D6 n3) – sharp-crested weir (0.42 m).

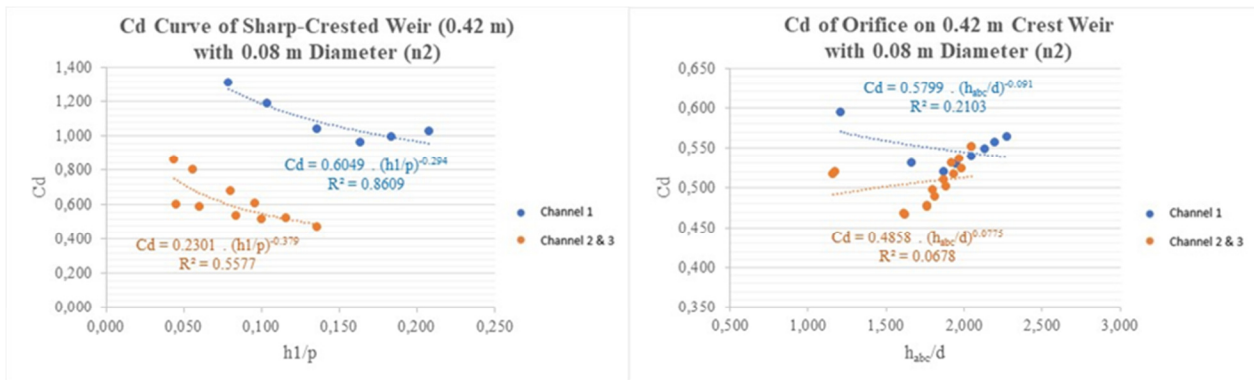


Fig. 20.  $C_d$  curve for sharp-crested weir and  $C_d$  for orifice (D8 n2) – sharp-crested weir (0.42 m).

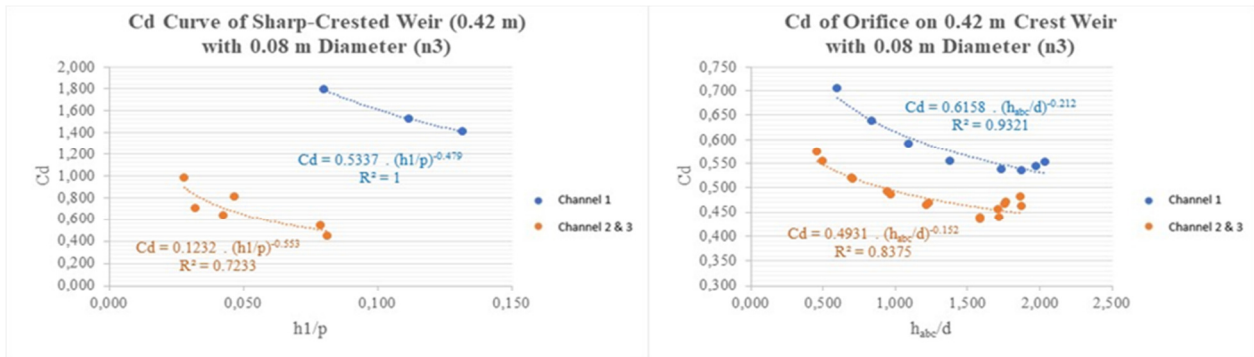


Fig. 21.  $C_d$  curve for sharp-crested weir and  $C_d$  for orifice (D4 n2) – sharp-crested weir (0.42 m).

TABLE IV. SUMMARY OF  $C_d$  MEAN, SHARP-CRESTED WEIR (0.33 m)

No.	Scenario	Mean of $C_d$ over sharp-crested weir			Mean	Mean of $C_d$ orifice			Mean
		Channel-1	Channel-2	Channel-3		Channel-1	Channel-2	Channel-3	
1.	Sharp-crested weir 0.33 m without orifice	0.860	0.751	0.797	0.803	-	-	-	-
2.	Sharp-crested weir 0.33 m combined with orifice D4 n2	0.810	0.519	0.563	0.631	0.546	0.514	0.515	0.525
3.	Sharp-crested weir 0.33 m combined with orifice D4 n3	0.847	0.508	0.554	0.636	0.549	0.517	0.515	0.527
4.	Sharp-crested weir 0.33 m combined with orifice D6 n2	0.871	0.440	0.486	0.599	0.570	0.537	0.535	0.548
5.	Sharp-crested weir 0.33 m combined with	1.016	0.408	0.482	0.635	0.568	0.524	0.528	0.540

No.	Scenario	Mean of $C_d$ over sharp-crested weir			Mean	Mean of $C_d$ orifice			Mean
		Channel-1	Channel-2	Channel-3		Channel-1	Channel-2	Channel-3	
	orifice D6 n3								
6.	Sharp-crested weir 0.33 m combined with orifice D8 n2	1.034	0.478	0.595	0.703	0.546	0.493	0.494	0.511
7.	Sharp-crested weir 0.33 m combined with orifice D8 n3	1.344	0.520	0.733	0.865	0.580	0.454	0.461	0.498

TABLE V. SUMMARY OF  $C_d$  MEAN, SHARP-CRESTED WEIR (0.42 m)

No.	Scenario	Mean of $C_d$ over sharp-crested weir			Mean	Mean of $C_d$ orifice			Mean
		Channel-1	Channel-2	Channel-3		Channel-1	Channel-2	Channel-3	
1.	Sharp-crested weir 0.42 m without orifice	0.928	0.839	0.889	0.885	-	-	-	-
2.	Sharp-crested weir 0.42 m combined with orifice D4 n2	0.821	0.540	0.576	0.646	0.559	0.534	0.535	0.543
3.	Sharp-crested weir 0.42 m combined with orifice D4 n3	0.905	0.510	0.556	0.657	0.557	0.524	0.524	0.535
4.	Sharp-crested weir 0.42 m combined with orifice D6 n2	0.929	0.466	0.498	0.631	0.567	0.538	0.537	0.547
5.	Sharp-crested weir 0.42 m combined with orifice D6 n3	1.068	0.475	0.596	0.713	0.558	0.515	0.519	0.531
6.	Sharp-crested weir 0.42 m combined with orifice D8 n2	1.088	0.542	0.687	0.772	0.548	0.506	0.511	0.521
7.	Sharp-crested weir 0.42 m combined with orifice D8 n3	1.573	0.595	0.777	0.982	0.582	0.479	0.487	0.516

Based on the summary of mean  $C_d$  from various scenarios with variations in the sharp-crested weir, orifice diameter, and number of orifices, the discharge coefficient ( $C_d$ ) for the sharp-crested weir at 0.42 m is greater than that at 0.33 m. For scenarios with a sharp-crested weir width of 0.33 m and 0.42 m, a greater orifice diameter in Channel-1 had a higher discharge coefficient. However, in Channel-2 and 3, the discharge coefficient fluctuates, which is also influenced by the number of orifices. For the variation of orifice number, a greater number of orifices causes a lower water overflow for the sharp-crested weir. This reduction in overflow increases the discharge coefficient. The variation of orifice diameter also influences the discharge coefficient. An increase in the orifice diameter reduces the overflow over the sharp-crested weir. During the experiments, it was observed that the water overflow over the sharp-crested weir increases as the discharge coefficient decreases.

When compared with previous studies, it is observed that practical applications, such as the use of stoplogs in off-take structures, present limitations despite their relatively simple construction. The installation and removal of stoplogs are labor-intensive and time-consuming, thereby reducing the operational efficiency. Prior research indicates that the average discharge coefficient ( $C_d$ ) for orifice weirs employed in such systems is approximately 0.894, which is notably higher than the  $C_d$  value of around 0.620 observed in tank-based orifice flow conditions.

In contrast, the present study reports that the mean  $C_d$  values for sharp-crested weirs combined with orifices range

between 0.5 and 0.8, depending on the configuration. These findings suggest that both structural design and operational mechanisms significantly affect discharge behavior and hydraulic performance.

TABLE VI. SUMMARY OF COEFFICIENT OF DETERMINATION ( $R^2$ ) FOR SHARP-CRESTED WEIR WITHOUT ORIFICE

Scenario of sharp-crested weir without orifice	Over sharp-crested weir	
	Channel-1	Channel-2 and 3
	$R^2$	$R^2$
Sharp-crested weir 0.33 m without orifice	0.9746	0.8927
Sharp-crested weir 0.42 m without orifice	0.9612	0.9528

To determine the extent of the independent variable's influence on the dependent variable, the determination coefficient ( $R^2$ ) is used. The coefficient of determination ( $R^2$ ) is a statistical measure that measures how well a regression model fits with the observed data. For the regression model of  $C_d$  over the sharp-crested weir, the relation between  $C_d$  and  $h/p$  is analyzed. Based on statistical analysis results, the most optimal regression model corresponds to the 0.33 m sharp-crested weir combined with orifices (3 units of 4 cm diameter each). However, for the 0.42 m sharp-crested weir combined with orifices, the configuration uses 3 units of 4 cm diameter orifices. For the sharp-crested weir without orifices, the most optimal regression model corresponds to the 0.42 m weir.

TABLE VII. SUMMARY OF COEFFICIENT OF DETERMINATION ( $R^2$ ) FOR SHARP-CRESTED WEIR OF 0.33 M

Scenario of sharp-crested weir of 0.33 m	Over sharp-crested weir		Orifice	
	Channel-1	Channel-2 and 3	Channel-1	Channel-2 and 3
	$R^2$	$R^2$	$R^2$	$R^2$
Sharp-crested weir 0.33 m combined with orifice D4 n2	0.4957	0.7935	0.9765	0.9242
Sharp-crested weir 0.33 m combined with orifice D4 n3	0.8580	0.7746	0.7025	0.8069
Sharp-crested weir 0.33 m combined with orifice D6 n2	0.1802	0.3914	0.9646	0.9389
Sharp-crested weir 0.33 m combined with orifice D6 n3	0.6628	0.5957	0.1328	0.4249
Sharp-crested weir 0.33 m combined with orifice D8 n2	0.9745	0.7652	0.3886	0.1880
Sharp-crested weir 0.33 m combined with orifice D8 n3	0.5698	0.6150	0.9111	0.3722

TABLE VIII. SUMMARY OF COEFFICIENT OF DETERMINATION ( $R^2$ ) FOR SHARP-CRESTED WEIR OF 0.42 M

Scenario of sharp-crested weir of 0.42 m	Over sharp-crested weir		Orifice	
	Channel-1	Channel-2 and 3	Channel-1	Channel-2 and 3
	$R^2$	$R^2$	$R^2$	$R^2$
Sharp-crested weir 0.42 m combined with orifice D4 n2	0.9411	0.8616	0.6274	0.8881
Sharp-crested weir 0.42 m combined with orifice D4 n3	0.9559	0.7436	0.9702	0.9787
Sharp-crested weir 0.42 m combined with orifice D6 n2	0.9683	0.5858	0.6793	0.9483
Sharp-crested weir 0.42 m combined with orifice D6 n3	0.9533	0.7981	0.2169	0.0183
Sharp-crested weir 0.42 m combined with orifice D8 n2	0.8609	0.5577	0.2103	0.0678
Sharp-crested weir 0.42 m combined with orifice D8 n3	1.0000	0.7233	0.9321	0.8375

## V. CONCLUSION

Based on the results, it can be concluded that in the Channel-1, which is the straight channel, the discharge coefficient is more than in the Channel-2 and 3 that are the turned channels. From the variation of sharp-crested weir width, the greater sharp-crested weir causes the bigger discharge coefficient. Regarding the orifice variation, the greater diameter of orifice causes the higher discharge coefficient, likewise for orifice number variation, the greater number of orifices causes a higher discharge coefficient.

Based on the statistical analysis, the regression model that gives more optimal and the biggest determination coefficient ( $R^2$ ) is in the sharp-crested weir of 0.33 m combined with the orifice of a 4 cm diameter and an orifice number of 2 units. However, in the sharp-crested weir of 0.42 m combined with orifice, the regression model that gives more optimal results is the orifice with a diameter of 4 cm and an orifice number of 3 units. For the sharp-crested weir without orifice, the regression model that gives more optimal results is the sharp-crested weir of 0.42 m width.

The novelty of this research lies in the unique overflow-orifice combination applied to a system with three distinct flow directions, which is not commonly addressed in previous studies. Additionally, a discharge coefficient model was constructed based on comprehensive physical tests and experimental data, providing a practical and empirically grounded insights for similar irrigation structures.

## REFERENCES

- [1] M. Tesfaye, S. Narain, and H. Muye, "Modeling of Water Distribution System for Reducing of Leakage," *Journal of Civil & Environmental Engineering*, vol. 10, no. 6, pp. 1–6, 2020.
- [2] R. Liemberger and A. Wyatt, "Quantifying the global non-revenue water problem," *Water Supply*, vol. 19, no. 3, pp. 831–837, May 2019, <https://doi.org/10.2166/ws.2018.129>.
- [3] T. Yu, X. Zhang, I. E. Lima Neto, T. Zhang, Y. Shao, and M. Ye, "Impact of Orifice-to-Pipe Diameter Ratio on Leakage Flow: An Experimental Study," *Water*, vol. 11, no. 10, Oct. 2019, Art. no. 2189, <https://doi.org/10.3390/w11102189>.
- [4] K. Ramamurthi and K. Nandakumar, "Characteristics of flow through small sharp-edged cylindrical orifices," *Flow Measurement and Instrumentation*, vol. 10, no. 3, pp. 133–143, Sep. 1999, [https://doi.org/10.1016/S0955-5986\(99\)00005-9](https://doi.org/10.1016/S0955-5986(99)00005-9).
- [5] P. Sharma and T. Fang, "Breakup of Liquid Jets from Non-circular Orifices," *Experiments in fluids*, vol. 55, no. 1, pp. 1–17, 2014.
- [6] J. F. Douglas, J. M. Gasiorek, and J. A. Swaffield, *Fluid mechanics*, 5th ed. Harlow, UK: Prentice Hall, 2001.
- [7] M. A. Al-Zahrani, "Modeling and Simulation of Water Distribution System: A Case Study," *Arabian Journal for Science and Engineering*, vol. 39, no. 3, pp. 1621–1636, Mar. 2014, <https://doi.org/10.1007/s13369-013-0782-z>.
- [8] J. R. Bermúdez, F.-R. López-Estrada, G. Besançon, G. Valencia-Palomo, and I. Santos-Ruiz, "Predictive Control in Water Distribution Systems for Leak Reduction and Pressure Management via a Pressure Reducing Valve," *Processes*, vol. 10, no. 7, Jul. 2022, Art. no. 1355, <https://doi.org/10.3390/pr10071355>.
- [9] N. Samir, R. Kansoh, W. Elbarki, and A. Fleifle, "Pressure control for minimizing leakage in water distribution systems," *Alexandria Engineering Journal*, vol. 56, no. 4, pp. 601–612, Dec. 2017, <https://doi.org/10.1016/j.aej.2017.07.008>.
- [10] M. T. Trinh, T. D. Nguyen, Q. T. Pham, A. N. Pham, and D. V. Dinh, "Hydro-Forming of U-Shaped Parts with Branches," *Engineering, Technology & Applied Science Research*, vol. 15, no. 1, pp. 19226–19231, Feb. 2025, <https://doi.org/10.48084/etasr.9227>.
- [11] D. N. Moriasi, J. G. Arnold, M. W. Van Liew, R. L. Bingner, R. D. Harmel, and T. L. Veith, "Model Evaluation Guidelines for Systematic Quantification of Accuracy in Watershed Simulations," *Transactions of the ASABE*, vol. 50, no. 3, pp. 885–900, 2007, <https://doi.org/10.13031/2013.23153>.
- [12] L. M. Asmelita, Limantara, M. Bisri, and W. Soetopo, "Rice Self-Sufficiency and Optimization of Irrigation by Using System Dynamic," *Civil Engineering Journal*, vol. 10, no. 2, pp. 489–501, 2024.
- [13] Y. C. Lim and D. S. Kim, *Hydraulic Design Practice of Canal Structures*. South Korea: Korea Rural Environmental Development Institute, 1981.
- [14] V. V. Ranade, V. M. Bhandari, S. Nagarajan, V. P. Sarvothaman, and A. A. Simpson, *Hydrodynamic cavitation: devices, design, and applications*, 1st ed. Weinheim, Germany: Wiley-VCH, 2023.
- [15] *Hydraulic Model Planning (Hydraulic Modeling)*. Yogyakarta, Indonesia: Hydraulics and Hydrology Laboratory, Center for Inter-University of Engineering Sciences, Gadjah Mada University, 1986.

- 
- [16] Y. Lian, I. C. Chan, J. Singh, M. Demissie, V. Knapp, and H. Xie, "Coupling of hydrologic and hydraulic models for the Illinois River Basin," *Journal of Hydrology*, vol. 344, no. 3–4, pp. 210–222, Oct. 2007, <https://doi.org/10.1016/j.jhydrol.2007.08.004>.
- [17] B. Triatmodjo, *Hydraulics II*, 2nd. ed. Indonesia: Beta Offset, 1995.
- [18] F. H. Richard, *Open-channel hydraulics*, 2nd. ed. New York: McGraw-Hill, 1994.
- [19] K. Subramanya, *Flow in open channels*, 5th. ed. Chennai: McGraw Hill Education (India), 2019.
- [20] K. G. Ranga Raju, *Flow through open channels*, 2nd. ed. New Delhi: Tata McGraw-Hill, 1993.
- [21] M. De Vries, *Scaling Model Hydraulic*. Delft, Netherlands: International Institute for Hydraulic and Environmental Engineering (IHE), 1982.